

TURBULENT DRAG REDUCTION BY POROUS COATINGS

N. Abderrahaman, R. Garcia-Mayoral

Department of Engineering, University of Cambridge, CB2 1PZ, Cambridge, UK

INTRODUCTION

In the present work we propose the use of anisotropically-porous coatings to reduce skin friction. Porous surfaces can produce an effectively slip for the overlying, turbulent flow. If the permeability of the porous layer is anisotropic, the apparent slip depends on the orientation of the flow with respect to the surface. In the case of riblets, the difference between the streamwise and spanwise slip lengths, $\ell_s = \ell_x - \ell_z$, was proposed as the controlling parameter for the drag reduction [12]. It was later shown that this is the case for any surface manipulation producing different ℓ_x and ℓ_z , and that for vanishing ℓ_s the drag reduction was proportional to its value expressed in wall units, with the proportionality constant being universal [9, 5, 11]. In agreement with the above, it was shown that porous surfaces can reduce friction if the substrate is permeable only in the streamwise direction [8].

The theoretical analyses in [12, 11, 9] predict that the drag reduction is proportional to the length-scale of the surface manipulations. However, this proportional trend begins to degrade for a given size, beyond which the performance ceases to improve, and the surface treatment is no longer interesting from an application perspective. In the case of riblets, this degradation occurs when Kelvin–Helmholtz-like spanwise rollers begin to develop over the surface [6]. These rollers generate additional Reynolds stresses, which are responsible for the degradation of drag. The same phenomenon has been shown to occur over plant canopies [4, 14], porous surfaces [1], and in general over obstructed, turbulent shear flows [7]. In the case of porous surfaces, this mechanism can be triggered by the wall-normal permeability alone [10].

Based on the above concepts of anisotropic slip length and onset of a Kelvin–Helmholtz-like instability, we aim to obtain estimates for the parameters that maximize the drag reduction produced by a coating with anisotropic porosity, like that sketched in figure 1. Such coating can be characterized by its thickness, h , and its streamwise, spanwise and wall-normal porosities, K_x , K_z and K_y . It is assumed that these are the principal directions of the porosity tensor, as in principle the pores should be elongated in the streamwise direction, in the spirit of [8], to maximize the longitudinal porosity while minimizing the transverse one.

SLIP EFFECT

To obtain the streamwise and spanwise effective slips, we consider the flow within the porous layer in response to an overlying, uniform shear. For small pore size, the problem reduces to solving the Brinkman equation [2, 16, 13] inside the porous medium, with no-slip conditions at the bottom of the porous layer and continuity of the tangential stress at the interface with the overlying free flow. The streamwise and

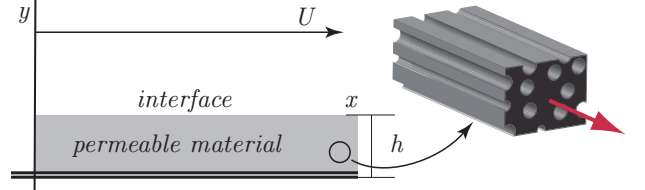


Figure 1: Schematic diagram of flow over an anisotropic porous surface.

spanwise slip lengths are then

$$\ell_x^+ \propto \sqrt{K_x^+} \tanh\left(h^+/\sqrt{K_x^+}\right), \quad (1)$$

$$\ell_z^+ \propto \sqrt{K_z^+} \tanh\left(h^+/\sqrt{K_z^+}\right). \quad (2)$$

The ‘+’ superscript indicates viscous-unit scaling. These relationships reveal that, in order to achieve a reduction in drag, the permeabilities should be $K_x > K_z$, as could have been intuitively predicted, but also that the coating thickness must be at least $h^+ \gtrsim \sqrt{K_x^+}$.

KELVIN–HELMHOLTZ INSTABILITIES

While the wall-normal permeability, K_y^+ , has no effect on ℓ_s^+ , if sufficiently large it can be responsible for a significant increase in drag [10]. As mentioned above, this increase can be traced to the triggering of a Kelvin–Helmholtz-like instability, which generates coherent spanwise rollers above the surface.

We focus now on the parameters controlling the development of this instability. Since Kelvin–Helmholtz instabilities are linear, inviscid processes, we look for solutions of the form $\exp[i(\alpha_x x + \alpha_z z - \omega t)]$ to the linearized Navier–Stokes equations, neglecting the viscous terms, as in [10], [14], and [6]. The Orr–Sommerfeld equations reduce then in essence to a Rayleigh problem, $(-\omega + \alpha_x U)(\partial^2/\partial y^2 - \alpha_x^2 - \alpha_z^2)v = \alpha_x U''v$, for which we use the same realistic $U(y)$ profiles of [3]. The instability develops because of the non-standard, impedance-like boundary condition that arises from the presence of a porous substrate, relating the pressure p and the wall-normal velocity v at the interface with the overlying flow. To obtain this condition we first solve the flow within the porous layer. Since the overlying perturbation flow is assumed to be inviscid, there is no shear transmitted to the flow within, which therefore follows simply Darcy’s equation. Imposing incompressibility and integrating along the coating depth h we obtain

$$v_0^+ = -[\tilde{\alpha}^+ \Phi_x K_y^+ \tanh(\tilde{\alpha}^+ \Phi_x h^+)] p_0^+, \quad (3)$$

where v_0 and p_0 represent the values of each v and p Fourier mode at the interface, $\tilde{\alpha} = (\alpha_x^2 + (K_z/K_x)\alpha_z^2)^{1/2}$ is the

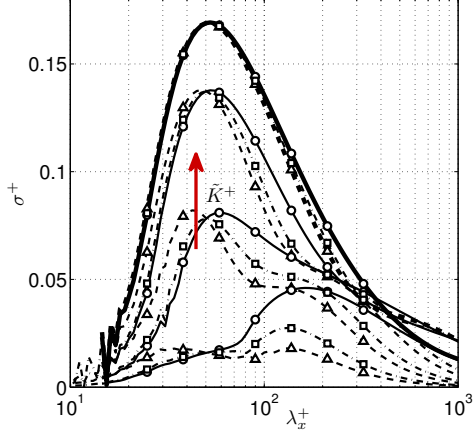


Figure 2: Growth rate σ^+ of the most amplified mode as a function of the longitudinal wavelength λ_x . $\tilde{K}^+ = 10^{[0.36, 0.82, 1.28, 2.20]}$ at $Re_\tau = 550$. —, $\Phi_x = 10^{-3}$, $h^+ = 10$; - - -, $\Phi_x = 10^3$, $h^+ = 10$; Δ , $\Phi_x = 1$, $h^+ = 1$; \circ , $\Phi_x = 1$, $h^+ = 100$; - \square -, $\Phi_x = 1$, $h^+ = 10$.

weighted wavenumber module, and $\Phi_x = (K_x/K_y)^{1/2}$ is the ratio between streamwise and wall-normal porosity lengths. Note that the boundary condition expressed in equation 3 represents a wavelength-dependent impedance, unlike that for a permeable medium in [10], but very similar to that used for riblets in [6], and somewhat connected to that of [15]. Provided that $K_x > K_z$, as recommended by the analysis of the slip effect, it can be shown that the most amplified mode is always longitudinal. The problem reduces then to a two-dimensional one with $\alpha_z = 0$.

The amplification $\sigma = \text{Im}(\omega)$ is shown in figure 2 as a function of the wavelength $\lambda_x = 2\pi/\alpha_x$ for base flows U at $Re_\tau = 550$. If both U and the boundary condition are expressed in wall units, the instability is essentially Re_τ -independent (not shown). The comparison with the analysis for a piecewise-linear profile shows that the length scales of the instability scale with the height y_c at which high values of U'' concentrate. For turbulent profiles, this height is $y_c^+ \approx 8$, independently of the Reynolds number [6]. The effect of the different coating parameters can then be essentially condensed into a single, reduced porosity parameter,

$$\tilde{K}^+ = K_y^+ \Phi_x \tanh\left(\Phi_x \frac{h^+}{y_c^+}\right), \quad (4)$$

as shown in figure 2. The results for different h^+ and Φ_x collapse quickly as \tilde{K}^+ increases, and are only significantly different for $\tilde{K}^+ < 5$. Nevertheless, the most amplified mode always consists of spanwise-homogeneous, streamwise-periodic rolling motions near the interface, which resemble those of [6], and for large \tilde{K}^+ the Kelvin-Helmholtz solution is always recovered.

The rapid development of the instability with \tilde{K}^+ is better appreciated in figure 3, which portrays σ^+ for the most amplified mode as a function of \tilde{K}^+ . The solution is in essence neutral for $\tilde{K}^+ \lesssim 1$ and fully developed for $\tilde{K}^+ \gtrsim 10$.

CONCLUSIONS

Some conclusions can be drawn from the above analysis on the expected drag behaviour of porous coatings. In order to achieve drag reduction, the streamwise permeability needs to be higher than the spanwise one, $K_x > K_z$, and the thickness of the coating must be $h^+ \gtrsim \sqrt{K_x^+}$. Under those conditions,

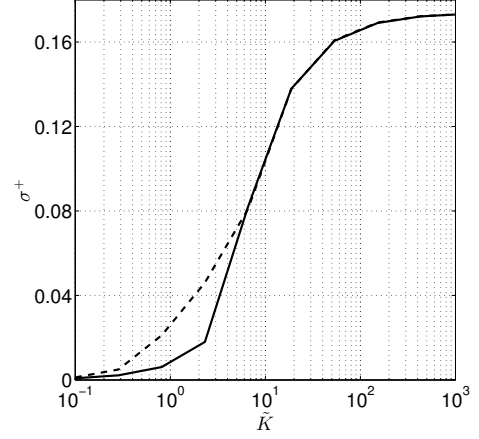


Figure 3: Maximum growth rate σ^+ as a function of the permeability \tilde{K}^+ at $Re_\tau = 550$. —, $\Phi_x = 10^{-3}$, $h^+ = 1$; - - -, $\Phi_x = 10^3$, $h^+ = 100$.

the drag reduction will be proportional to $\ell_s^+ \approx \sqrt{K_x^+} - \sqrt{K_z^+}$. However, this linear-with- ℓ_s^+ performance will begin to degrade eventually. In the most favourable case, $K_x > K_y$, this degradation will occur once $\tilde{K}^+ \approx (K_x^+ K_y^+)^{1/2} \approx 10$.

REFERENCES

- [1] W. P. Breugem, B. J. Boersma, and R. E. Uittenbogaard. *J. Fluid Mech.*, 562:35–72, 2006.
- [2] H. C. Brinkman. *Appl. Sci. Res. A*, 1:27–34, 1947.
- [3] J. C. del Álamo and J. Jiménez. *J. Fluid Mech.*, 559:205–213, 2006.
- [4] J. Finnigan. *Ann. Rev. Fluid Mech.*, 32:519–571, 2000.
- [5] R. García-Mayoral and J. Jiménez. *Phil. Trans. R. Soc. A*, 369:1412–1427, 2011.
- [6] R. García-Mayoral and J. Jiménez. *J. Fluid Mech.*, 678:317–347, 2011.
- [7] M. Ghisalberti. *J. Fluid Mech.*, 641:51–61, 2009.
- [8] S. Hahn, J. Je, and H. Choi. *J. Fluid Mech.*, 450:259–285, 2002.
- [9] J. Jiménez. *Phys. Fluids*, 6(2):944–953, 1994.
- [10] J. Jiménez, M. Uhlman, A. Pinelli, and Kawahara G. *J. Fluid Mech.*, 442:89–117, 2001.
- [11] P. Luchini. *ECCOMAS conference on numerical methods in engineering*, 465–470, 1996.
- [12] P. Luchini, F. Manzo, and A. Pozzi. *J. Fluid Mech.*, 228:87–109, 1991.
- [13] G. Neale and W. Nader. *Can. J. Chem. Eng.*, 52:475–478, 1974.
- [14] C. Py, E. de Langre, and B. Moulia. *J. Fluid Mech.*, 568:425–449, 2006.
- [15] C. Scalò, J. Bodart, S. K. Lele, and L. Joly. In *Proceedings of Summer Program 2014*, pages 305–314. Center of Turbulence Research, 2014.
- [16] G. I. Taylor. *J. Fluid Mech.*, 49:319–326, 1971.